European Review for Medical and Pharmacological Sciences 2020; 24: 4697-4709

Long noncoding RNA SNHG14 promotes malignancy of prostate cancer by regulating with miR-5590-3p/YY1 axis

Z.-F. LUO[1,2], Y. PENG[1,2], F.-H. LIU[1,2], J.-S. MA[1,2], G. HU[1,2], S.-L. LAI[1,2], H. LIN[1,2], J.-J. CHEN[1,2], G.-M. ZOU[1,2], Q. YAN[1,2], W.-G. SUI[1,2]

[1]The First School of Clinical Medicine, Southern Medical University, Guangzhou, Guangdong, China
[2]Department of Nephrology, Guangxi Key Laboratory of Metabolic Diseases Research, Affiliated No. 924 Military Hospital (Former No. 181 Military Hospital), Southern Medical University, Guilin, Guangxi, P.R. China

Zhi-Feng Luo and Ying Peng contributed to this paper equally

Abstract. – OBJECTIVE: Studies have demonstrated that long non-coding RNAs (lncRNAs) are important in the development and prognosis of prostate cancer. The aim of this study was to investigate the functions and mechanism of lnc-SNHG14 in prostate cancer.

PATIENTS AND METHODS: Quantitative Real Time-Polymerase Chain Reaction (qRT-PCR) or Western blot (WB) were performed to detect mRNA expressions of SNHG14 and miR-5590-3p, and the protein levels of Yin Yang-1 (YY1) in prostate cancer tissues, adjacent tissues, and cancer cell lines. The correlation analysis was used to analyze the correlations between SNHG14, miR-5590-3p, and YY1. Kaplan-Meier survival analysis was used to analyze the overall survival for prostate cancer patients. Cell Counting Kit-8 (CCK-8) assay was performed to measure cell proliferation ability and flow cytometry assay was used to detect cell apoptotic rate. Besides, transwell assay was used to measure cell invasion ability. In addition, WB was performed to measure protein expressions in prostate cancer cell lines. Finally, Luciferase reporter assay was performed to verify the binding sites between SNHG14 and miR-5590-3p, miR-5590-3p, and YY1.

RESULTS: The results showed that SNHG14 was significantly increased in prostate cancer tissues and prostate cancer cell lines, which were related with advanced stage and poor diagnosis for prostate cancer patients. MiR-5590-3p was reduced in prostate cancer tissues and cell lines, which were negatively correlated with SNHG14. YY1 was found to be increased in prostate cancer tissues, which was negatively correlated with miR-5590-3p and positively correlated with SNHG14. Furthermore, SNHG14 knockdown inhibited cell proliferation, invasion, and promoted cell apoptosis in DU145 cells. In addition, protein expressions of Cyclin D1, Bcl-2, and N-cadherin were repressed, and the levels of Bax, Cleaved Caspase-3, and E-cadherin were increased. Besides, miR-5590-3p inhibition promoted cell proliferation and invasion, and inhibited apoptosis in DU145 cells. Importantly, Luciferase reporter assay proved that SNHG14 could directly sponge with miR-5590-3p, which could bind with YY1 and regulate the functions of cancer cell. Finally, we proved that SNHG14 regulated cell proliferation, cell apoptosis, and invasion via miR-5590-3p/ YY1 axis in prostate cancer.

CONCLUSIONS: Above all, we found that SNHG14 was increased in prostate cancer patients, which was related with future diagnosis for prostate cancer patients. Of note, we discovered that SNHG14 could promote cell proliferation, invasion, and repress cell apoptosis *via* miR-5590-3p/YY1 axis in prostate cancer, which might provide a new target for treating prostate cancer.

Key Words:
Lnc-SNHG14, MiR-5590-3p, YY1, Cell invasion, Apoptosis, Prostate cancer.

Introduction

Prostate cancer is an epithelial malignancy in prostate, which is one of most common cancers in urinary system. The incidence of prostate cancer in China is increasing after the age of 55, which ranks the sixth of male malignant cancers[1-4]. Prostate cancer is mainly treated with androgen deprivation therapy, surgery, and radiotherapy[1,2]. However, the efficacy and outcome for prostate cancer patients are still unsatisfied, so new methods for early diagnosis and treatment are needed.

Most non-coding transcripts longer than 200 nt are known as long non-coding RNAs (ln-

Corresponding Author: Wei-Guo Sui, MD; e-mail: suiwg@163.com

cRNAs), which have been found[8-11] to play important roles in various cancers[5-7], including prostate cancer. Lnc-NEAT1 promoted resistance by sponging with miR-34a-5p and miR-204-5p in prostate cancer[8]; lnc-CASC15 was reported to promote cancer cell migration and invasion *via* targeting miR-200a-3p in prostate cancer[9]; lnc-MEG3 might act as a tumor suppressor to inhibit progression by modulating miR-9-5p/QKI-5 axis in prostate cancer[10].

Small nucleolar RNA host gene 14 (SNHG14) is a lncRNA that has been reported to play oncogenic functions, which could promote cancer cell proliferation, initiation, invasion, and migration in multiple cancers[12-15], including hepatocellular cancer[12], non-small cell lung cancer[13], cervical cancer[14], and colorectal cancer[15]. However, the functions of SNHG14 in prostate cancer have never been found.

MicroRNAs (miRNAs) are short RNAs that have been reported[16-18] to affect different functions in various tumors, including prostate cancer[8-11]. LncRNAs can sponge with miRNAs through endogenous RNA (ceRNA) mechanism and regulate biological functions in different cancers[19-22].

MiR-5590-3p was reported to play as a tumor-suppressive gene that could inhibit cancer cell proliferation and migration[23-25]. It was demonstrated that miR-5590-3p could inhibit tumor growth by targeting DDX5/AKT/m-TOR pathway in gastric cancer[23]; miR-5590-3p could regulate the proliferation and migration of triple-negative breast cancer[24]; miR-5590-3p was involved in tumor growth and metastasis in hepatocellular carcinoma[25]. However, the functions of miR-5590-3p in prostate cancer has not been studied.

This paper investigated SNHG14 expressions in prostate cancer tissues and prostate cancer cell lines. Thus, we explored the functions and potential mechanism of SNHG14 in prostate cancer patients.

Patients and Methods

Clinical Patient Samples

60 cases of prostate cancer tissue samples and the adjacent tissue samples were collected by surgical resection from August 2012 to September 2013 in our hospital. The samples were frozen at -80°C. Clinical features of prostate cancer patients were listed in Table I. This study was approved by the Faculty of Medicine's Ethics Committee of our hospital and every patient signed the informed consent.

Cell Culture

Normal human myofibroblast stromal cell (WPMY1) and human prostate cancer cell lines, including LNCaP, 22RV1, PC-3, and DU145, were purchased from the American Type Culture Collection (ATCC; Manassas, VA, USA). The cells were cultured in Dulbecco's Modified Eagle's Medium

Table I. The relationships between SNHG14 expression and clinical characters in patients with prostate cancer.

Parameters	No.	Low SNHG14	High SNHG14	*p*-value
Total patients	60	30	30	
Age				0.580
< 65Y	19	8	11	
≥ 65Y	41	22	19	
Tumor size				0.037
< 3 cm	33	21	12	
≥ 3 cm	27	9	18	
Lymph node metastasis				0.019
Yes	32	11	21	
No	28	19	9	
Distant metastasis				0.170
Yes	20	7	13	
No	40	23	17	
Histological grade				0.004
Well and moderately	28	20	8	
Poorly and others	32	10	22	
TNM stage				0.035
I-II	25	17	8	
III-IV	35	13	22	

(DMEM)/F12 medium (Invitrogen, Carlsbad, CA, USA) containing with 10% fetal bovine serum (FBS; Gibco, Rockville, MD, USA). The cells were cultured in an incubator with 5% CO_2 at 37°C.

Construction of siRNA and Cell Transfection

Small interfering RNA (siRNA) for SNHG14 was synthesized and constructed into a plasmid. SiRNA negative control (si-NC) was obtained from Invitrogen (Invitrogen, Carlsbad, CA, USA). The cells were pre-incubated on 6-well plates until about 50% confluence, and then, si-SNHG14 and si-NC were respectively transfected with Lipofectamine 2000 (Invitrogen, Carlsbad, CA, USA) following the protocol. The stable cells with SNHG14 inhibition were obtained after one week. In the other way, indicated cells were pre-incubated on 6-well plates until about 70%, then, miR-NC or miR-5590-3p inhibitor was transfected into cells with Lipofectamine 2000, according to the protocol.

CCK-8 Assay

Cell Counting Kit-8 assay (CCK-8, Dojindo Molecular Technologies, Kumomoto, Japan) was used to measure cell proliferation ability following the protocol. The cells were pre-incubated on 96-well plates for 0 h, 24 h, 48 h, and 72 h, then, 10 µl CCK-8 was added and incubated for other 2 h. The optical density (OD) value was measured at 450 nm with microplate reader (Thermo Fisher Scientific, Waltham, MA, USA).

Flow Cytometry for Cell Apoptosis Analysis

Flow cytometry was used to analyze the cell apoptotic rate. The treated DU145 cells were digested with trypsin and fixed. The pellet was stained with FITC-Annexin V and Propidium Iodide (PI), and then, flow cytometry was performed within 5 mins. The apoptotic cells were obtained using a FACSCalibur system (BD Biosciences, Franklin Lakes, NJ, USA), and images were analyzed by FlowJo software (Tree Star Corp, Ashland, OR, USA).

Transwell Assay

Transwell assay was used to measure cell invasion ability, 24-well transwell chamber (Costar, Cambridge, MA, USA) was used in this assay. The cells were seeded with serum-free DMEM/F12 in the upper chamber, and the lower chambers were filled with DMEM/F12 containing 20% FBS to induce cell invasion. After culturing for 48 h, non-invasive cells were removed, and the ells invaded through the membranes were stained with 0.1% crystal violet (Biyuntian, Shanghai, China). At least four random fields were counted in each chamber with an inverted light microscope (Olympus Corporation, Tokyo, Japan).

RNA Extraction and quantitative Real Time-PCR

Total RNA was isolated from human samples and prostate cancer cell lines by TRIzol reagent (Invitrogen, Carlsbad, CA, USA) according to the protocol and purified by GeneJET RNA Purification Kit (Thermo Fisher Scientific, Waltham, MA, USA). Total RNA was reversed by PrimeScript™ RT reagent Kit (TaKaRa, Dalian, China) according to the manufacturer's protocol. The primers for qRT-PCR were synthesized by Gene Pharma (Shanghai, China), which were listed in Table II. The mRNA expressions were measured by SYBR® Premix DimmerEraser™ kit (TaKaRa, Dalian, China) and the relative mRNA expressions were calculated by $2^{-\Delta\Delta CT}$ method. GAPDH or U6 was used for normalization.

Western Blot

Total protein was extracted from human samples and prostate cancer cells using a RIPA lysis

Table II. Primers for qRT-PCR.

Gene names	Primer sequences
SNHG14	Forward: 5'-GGGTGTTTACGTAGACCAGAAC-3' Reverse: 5'-CTTCCAAAAGCCTTCTGCCTTAG-3'
miR-5590-3p	Forward: 5'-CCCCCTTGTCATGTTCCTGATCTT-3' Reverse: 5'-GCAGAGGAAATGAAACCAGTATG-3'
GAPDH	Forward: 5'-CGGAGTCAACGGATTTGGTCGTAT-3' Forward: 5'-AGCCTTCTCCATGGTGGTGAAGAC-3'
U6	Forward: 5'-CGCTTCGGCAGCACATATACT-3' Forward: 5'-CGCTTCACGAATTTGCGTGTC-3'

buffer (Beyotime, Shanghai, China). 40 mg of proteins were separated by 10% sodium dodecyl sulphate-polyacrylamide gel electrophoresis (SDS-PAGE), and then, transferred onto polyvinylidene difluoride (PVDF) membranes (Millipore, Billerica, MA, USA). After blocking with 5% nonfatty milk at room temperature for 1 h, the membranes were incubated with primary antibodies overnight at 4°C, including YY1 (ab109237, Abcam, Cambridge, MA, USA, 1:5000, 45 kDa), Cyclin D1 (ab134175, Abcam, Cambridge, MA, USA, 1:5000, 34 kDa), Bcl-2 (ab97051, Abcam, Cambridge, MA, USA, 1:1000, 26 kDa), Bax (ab32503, Abcam, Cambridge, MA, USA, 1:5000, 21 kDa), Cleaved Caspase-3 (ab2302, Abcam, Cambridge, MA, USA, 1:1000, 17 kDa), N-cadherin (ab18203, Abcam, Cambridge, MA, USA, 1:1000, 100 kDa), E-cadherin (ab40772, Abcam, Cambridge, MA, USA, 1:5000, 97 kDa), and GAPDH (ab8245, Abcam, Cambridge, MA, USA, 1:5000, 36 kDa). Then, the membranes were incubated with matched secondary antibodies for 1 h. The proteins were detected by enhanced chemiluminescence (ECL) reagents (Pierce, Rockford, IL, USA) with ECL detection system (Thermo Fisher Scientific, Waltham, MA, USA). The relative protein expressions were calculated and GAPDH was used for normalization.

Luciferase Reporter Assay

The pmiR-GLO Dual-Luciferase vectors (Promega, Madison, WI, USA) containing wild type SNHG14 (WT-SNHG14) and mutant SNHG14 (MUT-SNHG14) were constructed, and the vectors containing wild type YY1 (WT-YY1) and mutant YY1 (MUT- YY1) were also constructed. The cells were seeded on 48-well plates, the vectors were respectively co-transfected with miR-5590-3p mimic or miR-NC in DU145 cells with Lipofectamine 2000 according to the protocol. Activities of Firefly Luciferase and Renilla Luciferase were measured by Promega Luciferase Assay (Promega, Madison, WI, USA). Relative Luciferases were analyzed, and Renilla Luciferase gene was used for normalization.

Statistical Analysis

Data were presented as (mean± SD), and were analyzed by SPSS 22.0 (IBM Corp., Armonk, NY, USA) and GraphPad Prism 6.0 (GraphPad Software, La Jolla, CA, USA). The significance between the groups was analyzed by Student's *t*-test or one-way ANOVA and SNK method. Pearson correlation was utilized for verifying the significance of the correlation among SNHG14, miR-5590-3p, and YY1 in patient samples. Kaplan-Meier survival test was performed to analyze the overall survival. $p<0.05$ was considered as statistically significant.

Results

SNHG14 was Increased in Prostate Cancer Tissues and Prostate Cancer Cell Lines

To investigate SNHG14 expressions in prostate cancer tissues, sixty paired prostate cancer tissues and adjacent tissues were collected and SNHG14 expressions were detected by qRT-PCR. The results showed that SNHG14 was increased in prostate cancer tissues, compared to adjacent tissues (Figure 1A) ($p<0.001$). Furthermore, SNHG14 expression in patients at stage III-IV was higher than that of patients at stage I-II (Figure 1B) ($p<0.001$). The clinical characters of prostate cancer patients were listed in Table I, which revealed that SNHG14 high expression was related with tumor size, lymph node metastasis, histological grade, and advanced stages (Table I) ($p<0.05$). Additionally, Kaplan-Meier survival illustrated that patients with SNHG14 high expression showed a lower overall survival rate (Figure 1C) ($p<0.05$). To investigate the mechanism of SNHG14 in prostate cancer, we detected SNHG14 expressions in prostate cancer cell lines, which showed that SNHG14 expressions were increased (Figure 1D) ($p<0.01$). These data suggested that SNHG14 was increased in prostate cancer tissues, which was related with future diagnosis of prostate cancer patients. However, the underlying functions of SNHG14 in prostate cancer remained unclear.

SNHG14 Downregulation Repressed Cell Proliferation, Invasion, and Promoted Apoptosis in DU145 Cells

In order to study the functions of SNHG14 in prostate cancer, SNHG14 si-RNA was constructed into a plasmid (si-SNHG14). After si-SNHG14 or si-NC was transfected into DU145 cells, we found that SNHG14 was significantly inhibited, compared with control and si-NC (Figure 2A) ($p<0.001$). CCK-8 assay revealed that SNHG14 downregulation repressed cell proliferation (Figure 2B) ($p<0.01$). Flow cytometry results revealed that SNHG14 downregulation promoted cell apoptosis (Figure 2C) ($p<0.01$). Furthermore, transwell assay showed that SNHG14 downregulation re-

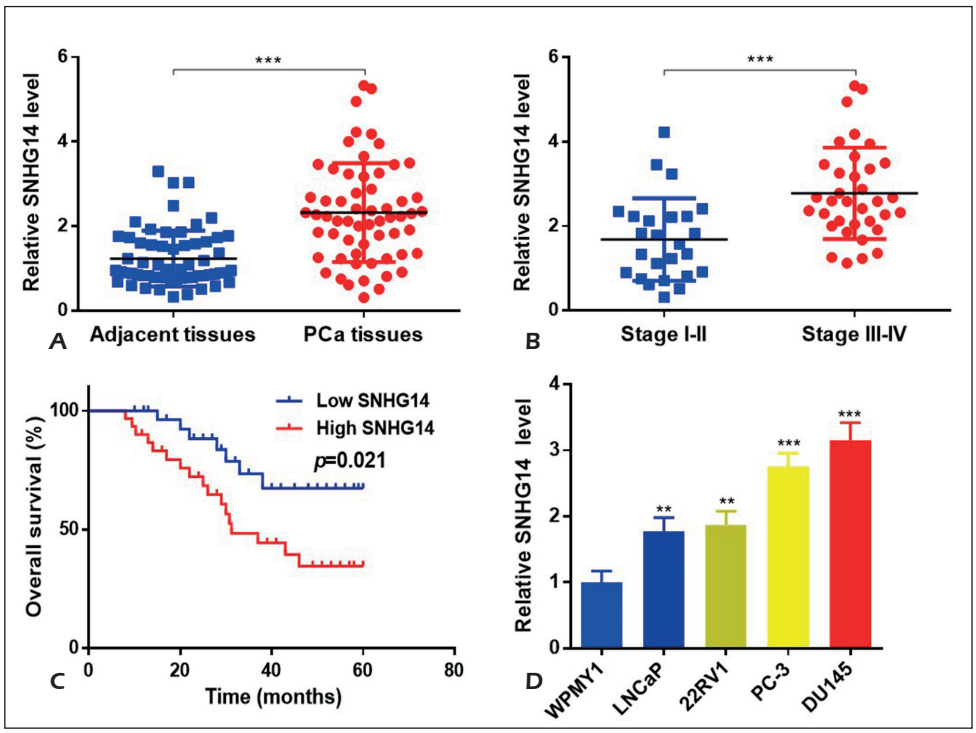

Figure 1. SNHG14 was increased in prostate cancer tissues and prostate cancer cell lines. **A**, SNHG14 expressions in prostate cancer tissues (n=60) and adjacent tissues (n=60) were detected by qRT-PCR. **B**, SNHG14 expressions in patients at stage I-II (n=25) and stage III-IV (n=35) were analyzed. **C**, Overall survival of prostate cancer patients was analyzed by Kaplan-Meier survival analysis. **D**, SNHG14 expressions in prostate cancer cell lines were detected. **p<0.01, ***p<0.001.

pressed cell invasion ability (Figure 2D) (p<0.01). In addition, we detected proliferation and apoptosis associated gene expressions, including Cyclin D1, Bcl-2, Bax, Cleaved caspase-3, and we also detected invasion associated gene expressions, including N-cadherin and E-cadherin. The results showed that the protein expressions of Cyclin D1, Bcl-2, and N-cadherin were repressed, while the levels of Bax, Cleaved caspase-3, and N-cadherin were promoted (Figure 2E, F) (p<0.01), further suggesting that SNHG14 downregulation repressed cell proliferation, invasion, and promoted apoptosis in DU145 cells. However, the detailed mechanism remained unclear.

MiR-5590-3p was Reduced in Prostate Cancer and it Could Directly Sponge with SNHG14 in DU145 Cells

To further understand the mechanism of SNHG14 in prostate cancer, we used bioinformatics analysis to explore the targets of SNHG14, and miR-5590-3p was predicted to have complementary binding sites, which was reported to be involved in the progression of some cancers[23-25]. We found that miR-5590-3p expression was decreased in prostate cancer tissues (Figure 3A) (p<0.001), and miR-5590-3p expression in patients at stage III-IV was lower than patients at stage I-II (Figure 3B) (p<0.001). In addition, correlation analysis revealed that miR-5590-3p was negatively correlated with SNHG14 in prostate cancer tissues (Figure 3C) (p<0.05) but not in adjacent tissues (Figure 3D) (p>0.05), especially in patients at stage of III-IV (Figure 3E) (p<0.01) but not in patients at stage of I-II (Figure 3F) (p>0.05). Besides, miR-5590-3p expressions were significantly reduced in prostate cancer cell lines, especially in DU145 cells (Figure 3G) (p<0.001) and they were increased following SNHG14 inhibition (Figure 3H) (p<0.001). Above all, these data prompted that SNHG14 was negatively interacted with miR-5590-3p, which was predicted as a downstream molecule for SNHG14. To verify whether miR-5590-3p could competitively sponge with SNHG14, wild type and mutant sequences of SNHG14 were constructed into GLO vectors (Figure 3I) and the Luciferase reporter assay was performed. The results demonstrated that the relative Luciferase activity in DU145 cells co-transfected with WT-SNHG14 and miR-5590-3p mimic was significantly repressed, while it was

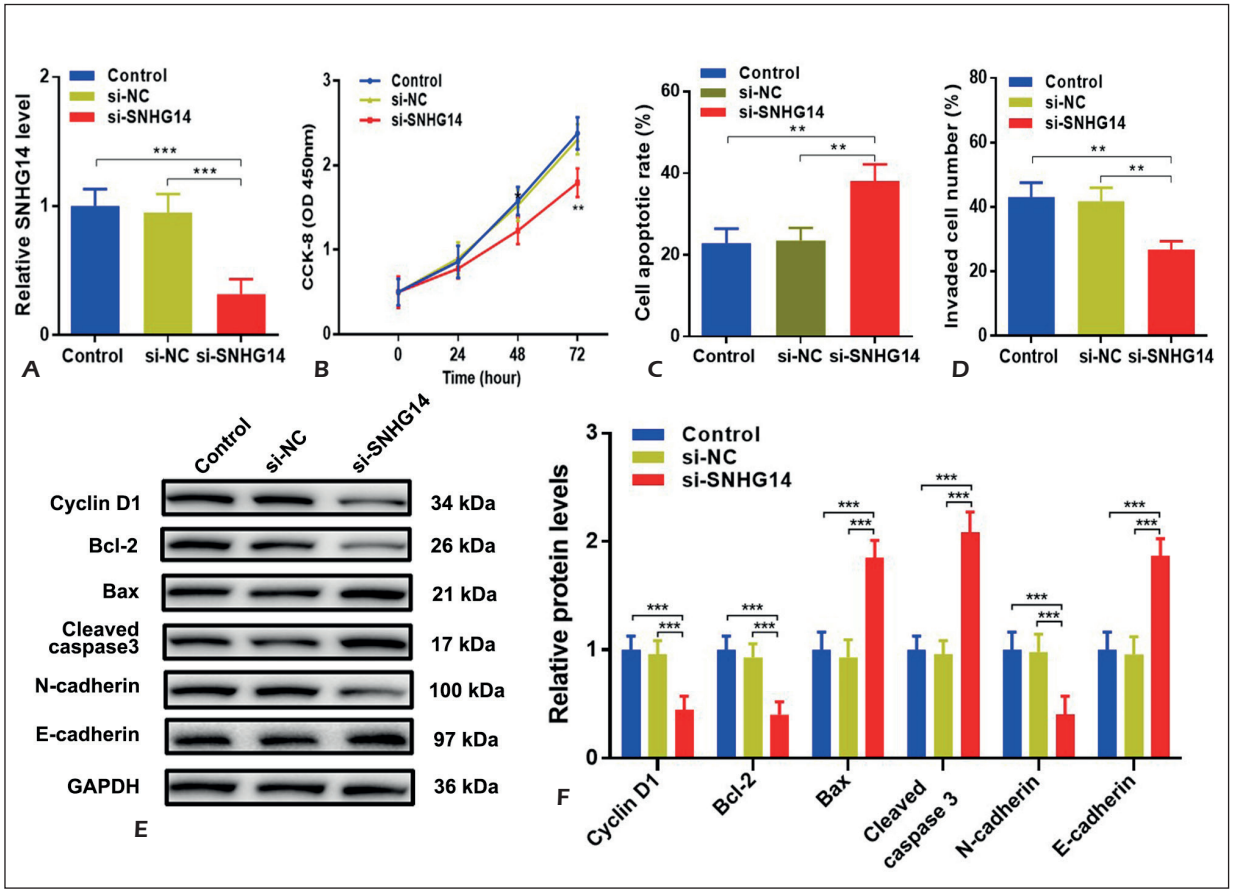

Figure 2. SNHG14 downregulation repressed cell proliferation, invasion and promoted apoptosis in DU145 cells. **A**, SNHG14 expressions were detected by qRT-PCR. **B**, Proliferation abilities were measured by CCK-8 assay. **C**, Cell apoptotic rate was evaluated by flow cytometry. **D**, Invasion abilities were measured by transwell assay. **E-F**, Protein levels of Cyclin D1, Bcl-2, Bax, Cleaved caspase-3, N-cadherin, and E-cadherin were detected by WB (magnifications: x2.0). **p<0.01, ***p<0.001.

reversed following co-transfection with MUT-SNHG14 (Figure 3J) (p<0.01). These data demonstrated that miR-5590-3p was reduced in prostate cancer and it could directly sponge with SNHG14 in DU145 cells.

MiR-5590-3p Downregulation Promoted Cell Proliferation, Invasion and Inhibited Apoptosis in DU145 Cells

To further explore how miR-5590-3p regulated prostate cancer cell functions, miR-5590-3p inhibitor or miR-NC was respectively transfected into DU145 cells, which revealed that miR-616-5p was significantly decreased in miR-5590-3p inhibitor group (Figure 4A) (p<0.001). CCK-8 assay prompted that cell proliferation ability was improved following miR-5590-3p inhibition (Figure 4B) (p<0.001). Flow cytometry revealed that miR-5590-3p downregulation repressed cell apoptosis (Figure 4C) (p<0.01). Transwell assay showed that cell invasion ability was improved following miR-5590-3p inhibition (Figure 4D) (p<0.01). Moreover, WB showed that the protein expressions of Cyclin D1, Bcl-2, and N-cadherin were increased, while the levels of Bax, Cleaved caspase-3, and N-cadherin were repressed (Figure 4E, F) (p<0.001), which further verified that miR-5590-3p downregulation promoted cell proliferation, invasion, and inhibited apoptosis in DU145 cells. However, the detailed mechanism of miR-5590-3p in prostate cancer was unclear.

MiR-5590-3p Could Directly Target at Binding with YY1

To explore how miR-5590-3p promoted cell proliferation, invasion, and inhibited apoptosis in prostate cancer, TargetScan database was used to predict the target genes with 3'UTR. YY1, an oncogene to

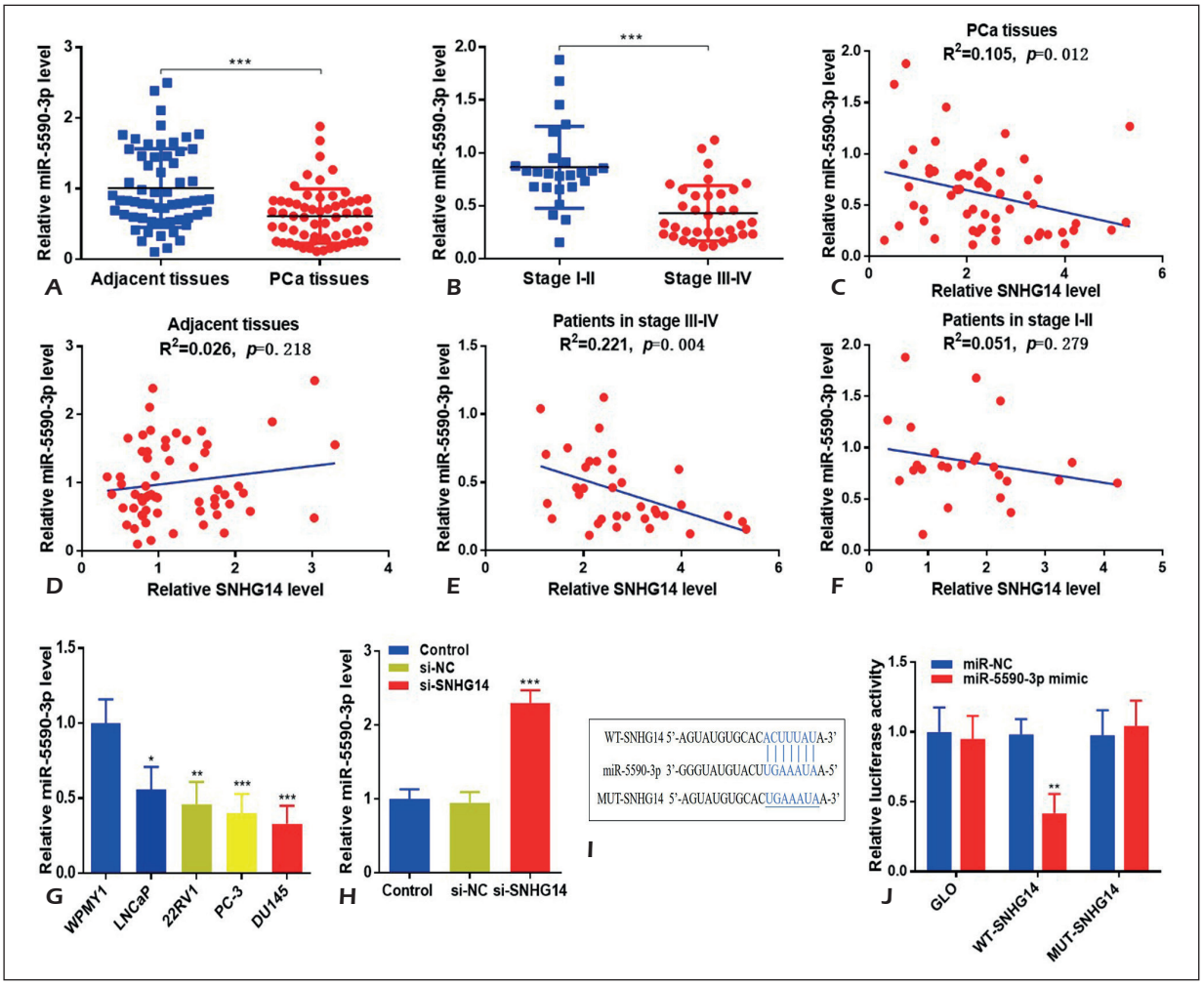

Figure 3. MiR-5590-3p was reduced in prostate cancer and it could directly sponge with SNHG14 in DU145 cells. **A**, MiR-5590-3p expressions in prostate cancer tissues (n=60) and adjacent tissues (n=60) were detected. **B**, MiR-124-3p expressions in patients at stage I-II (n=25) and stage III-IV (n=35) were analyzed. **C-D**, Correlations between SNHG14 and miR-5590-3p were analyzed in prostate cancer tissues and adjacent tissues. **E-F**, Correlations between SNHG14 and miR-5590-3p were analyzed in patients at stage I-II and stage III-IV. **G-H**, MiR-5590-3p expressions were detected in prostate cancer cell lines and in DU145 cells transfected with si-SNHG14 or si-NC. **I**, Wild type and mutant sequences of SNHG14 were synthesized. **J**, Luciferase gene reporter assay was performed in DU145 cells. *p<0.05, **p<0.01, ***p<0.001.

promote progression in some cancers[26-29], was identified to be a potential target gene of miR-5590-3p. Then, we detected the protein expressions of YY1 in human prostate cancer tissues and adjacent tissues by WB. The results showed that YY1 protein expression was significantly increased in prostate cancer tissues (Figure 5A) (p<0.001) and the expression level in patients at stage III-IV was much higher than these at stage I-II (Figure 5B) (p<0.001). Furthermore, correlation analysis revealed that miR-5590-3p was negatively correlated with YY1 in prostate cancer tissues and patients at stage of III-IV(Figure 5C, E) (p<0.01), but not in adjacent tissues and patients at stage of I-II (Figure 5D, F) (p>0.05). Moreover, YY1 protein levels in prostate cancer cell lines were increased (Figure 5G) (p<0.05).

Above all, these data demonstrated that miR-5590-3p was negatively correlated with YY1, which might be a target of miR-5590-3p. To understand whether miR-5590-3p could bind with YY1 in prostate cancer, plasmids with YY1 wild type and mutant sequences were synthesized and Luciferase gene reporter assay was carried out (Figure 5H). Results showed that miR-5590-3p mimic sig-

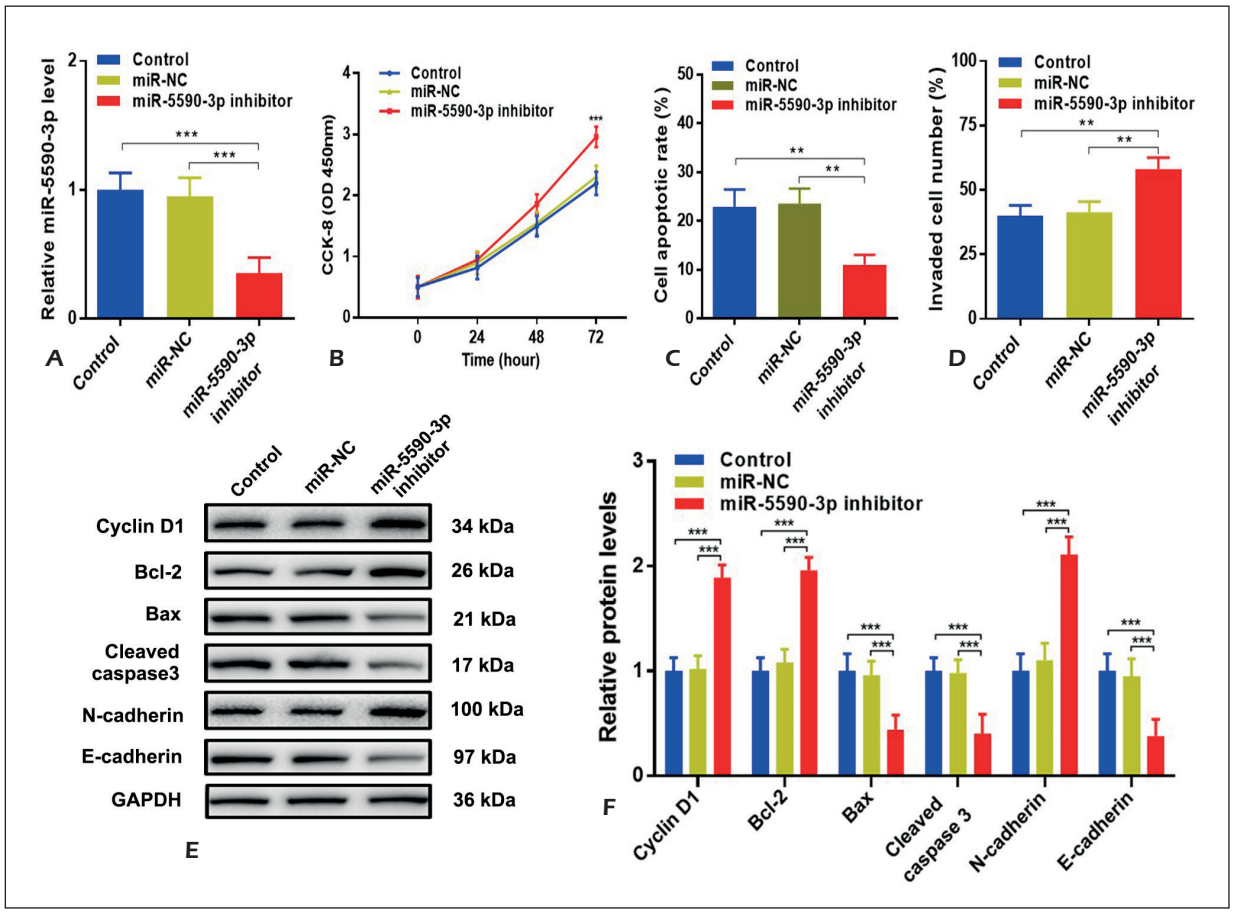

Figure 4. MiR-5590-3p downregulation promoted cell proliferation and invasion, and inhibited apoptosis in DU145 cells. **A**, MiR-5590-3p expressions were detected after miR-5590-3p inhibitor transfection. **B**, CCK-8 assay was performed to measure cell proliferation ability. **C**, Cell apoptotic rate was evaluated by flow cytometry. **D**, Invasion abilities were measured by transwell assay. **E-F**, Protein levels of Cyclin D1, Bcl-2, Bax, Cleaved caspase-3, N-cadherin, and E-cadherin were detected by WB (magnifications: x2.0). ***p<0.001.

nificantly reduced the Luciferase activity of YY1-WT but not in that of YY1-MUT vector in DU145 cells (Figure 5I) (p<0.01). Collectively, above data suggested that miR-5590-3p could bind with YY1 and regulate cancer cell biological features.

SNHG14 was Positively Interacted with YY1 in Prostate Cancer Tissues

We demonstrated that SNHG14 could sponge with miR-5590-3p, which would bind with YY1, and the correlation analysis was performed to make a clear understanding between SNHG14 and YY1. Results showed that SNHG14 was positively correlated with YY1 in prostate cancer tissues, as well as in patients at stage of III-IV (Figure 6A, C) (p<0.05), but not in adjacent tissues and patients at stage of I-II (Figure 6B, D) (p>0.05). Furthermore, YY1 protein expression was reduced in SNHG14 inhibition group in DU145 cells (Figure 6E) (p<0.01). These data indicated that SNHG14 was positively interacted with YY1 in prostate cancer tissues. Therefore, we assumed that SNHG14 could function as a ceRNA to sponge with miR-5590-3p, which would directly repress YY1 expression and regulate cancer cell biological features in prostate cancer.

SNHG14 Regulated Cancer Cell Growth, Apoptosis and Invasion Via MiR-5590-3p/ YY1 Axis in Prostate Cancer

Based on above data, we might confirm that SNHG14 could function as a ceRNA to sponge with miR-5590-3p, which would repress YY1 expression. To validate our assumption, miR-5590-3p inhibitor was transfected into DU145 cells with si-SNHG14 or si-NC. Results showed that SNHG14

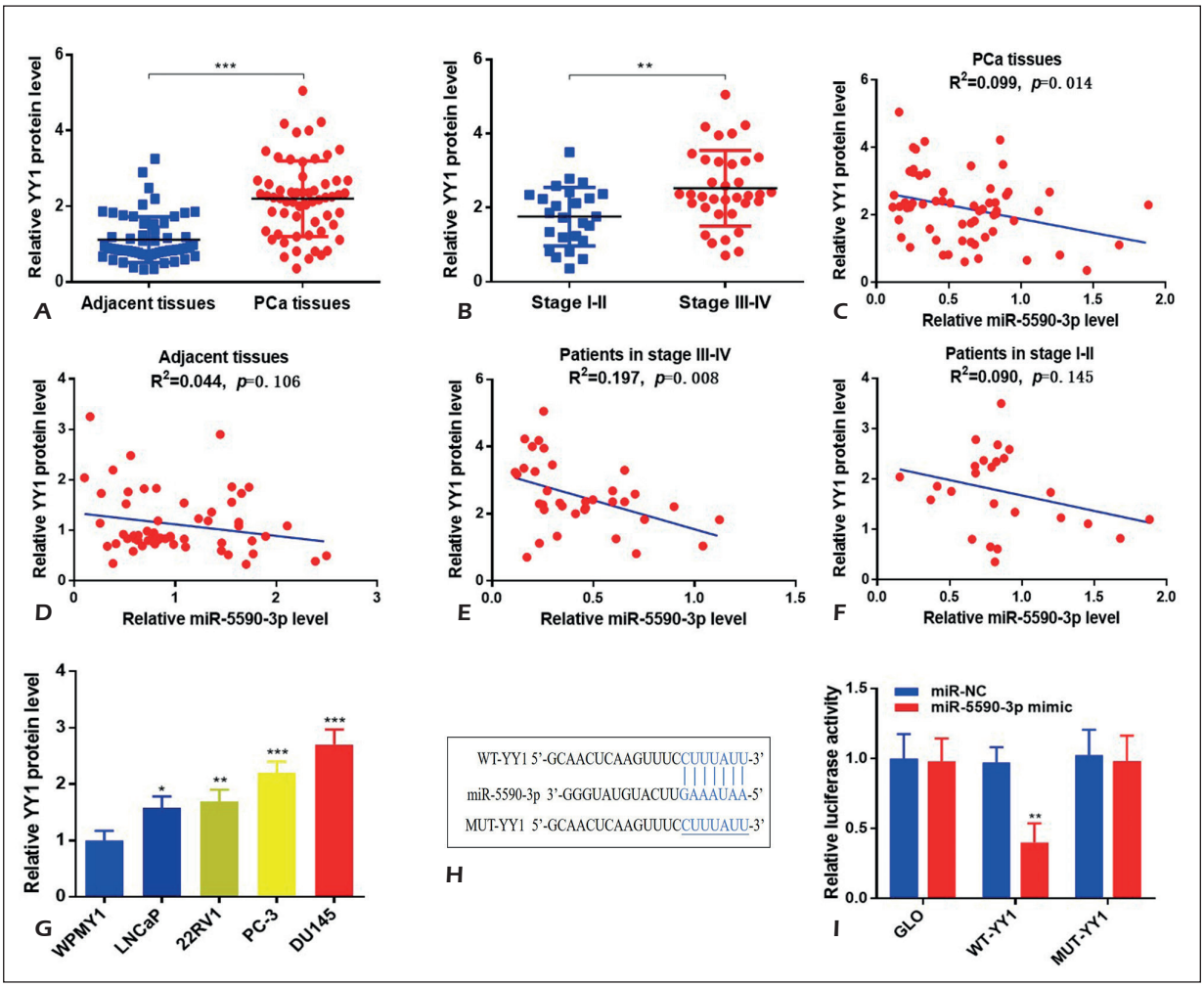

Figure 5. MiR-5590-3p could directly target at binding with YY1. **A**, YY1 protein levels in prostate cancer tissues (n=60) and adjacent tissues (n=60) were detected by WB. **B**, YY1 protein levels in patients at stage I-II (n=25) and stage III-IV (n=35) were analyzed. **C-D**, Correlations between YY1 and miR-5590-3p were analyzed in prostate cancer tissues and adjacent tissues. **E-F**, Correlations between YY1 and miR-5590-3p were analyzed in patients at stage I-II and stage III-IV. **G**, YY1 protein levels were detected in prostate cancer cell lines. **H**, Plasmids with YY1 wild type and mutant sequences were synthesized. **I**, Luciferase gene reporter assay was performed in DU145 cells. *p<0.05, **p<0.01, ***p<0.001.

was reduced and miR-5590-3p was increased in cells with si-SNHG14. SNHG14 and miR-5590-3p were both reversed following miR-5590-3p inhibitor transfection (Figure 7A) (p<0.001). CCK-8 assays indicated that miR-5590-3p inhibition could promote the repressed cell proliferation ability in cells with si-SNHG14 (Figure 7B) (p<0.01). Flow cytometry revealed that miR-5590-3p inhibition could repress the promoted cell apoptosis in the cells with si-SNHG14 (Figure 7C) (p<0.01). Besides, transwell assay illustrated that the restrained invasion effect of SNHG14 inhibition was countervailed by miR-5590-3p inhibition in DU145 cells (Figure 7D) (p<0.001). In addition, WB showed that SNHG14 inhibition repressed protein expressions of YY1, Cyclin D1, Bcl-2, N-cadherin, and increased Bax, Cleaved caspase-3, and E-cadherin expression, while they were countervailed by miR-5590-3p inhibition (Figure 7E, F) (p<0.001). Above all, these results confirmed that SNHG14 regulated cancer cell growth, apoptosis, and invasion *via* miR-5590-3p/YY1 axis in prostate cancer.

Discussion

Prostate cancer is one of the most malignant cancers in the urinary system, which ranks the

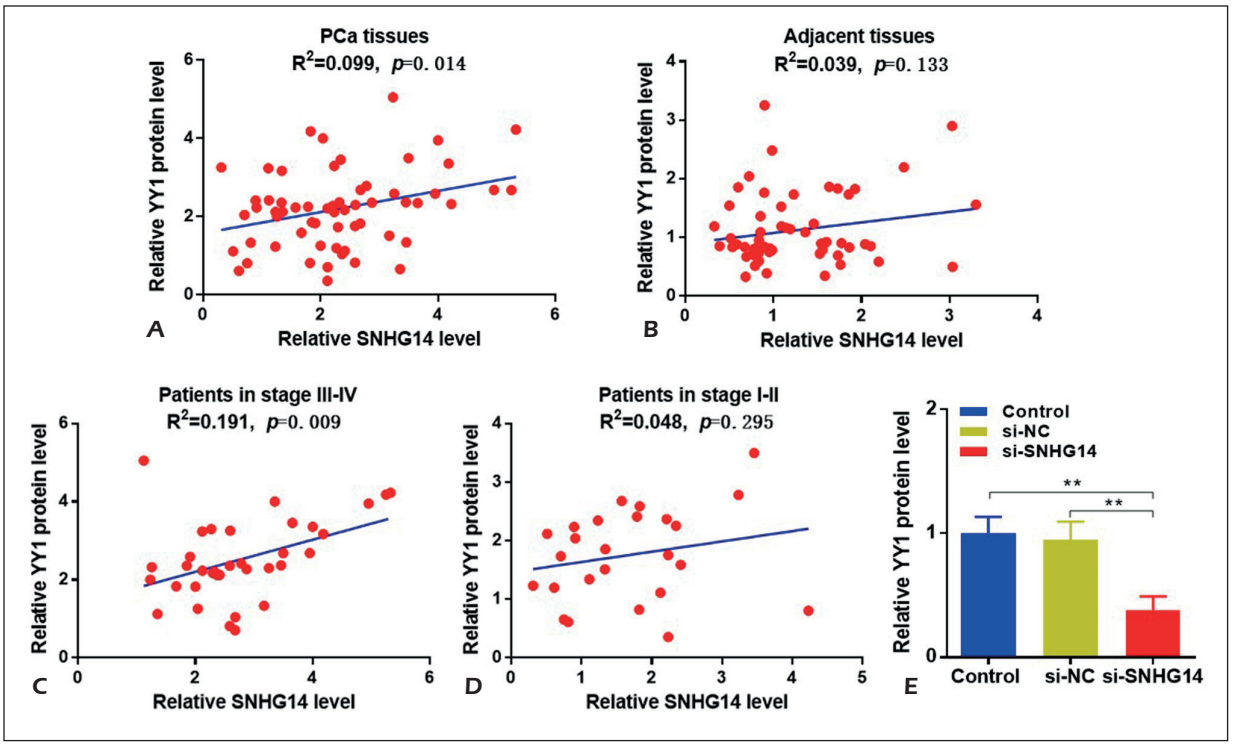

Figure 6. SNHG14 was positively interacted with YY1 in prostate cancer tissues. **A-B**, Correlation between SNHG14 and YY1 was analyzed in prostate cancer tissues and adjacent tissues. **C-D**, Correlation between SNHG14 and YY1 was analyzed in prostate cancer patients at stage III-IV and stage I-II. **E**, YY1 protein expressions were detected by WB. $^{**}p<0.01$.

sixth of male malignant cancers[1-4]. Although new diagnosis and treatment methods have been applied in prostate cancer, the future outcomes for prostate cancer patients are still unsatisfied. As a result, we wanted to reach a better understanding of prostate cancer and find novel methods for prostate cancer.

LncRNAs are kinds of long RNAs that play important roles in various cancers[5-7], including prostate cancer[8-11]. SNHG14 has been reported to be an oncogene, which can promote cancer cell proliferation, initiation, invasion, and migration in cancers[12-15]. However, the functions of SNHG14 in prostate cancer have not been studied. For the first time, we detected SNHG14 expressions in prostate cancer tissues and prostate cancer cell lines. Results showed that SNHG14 was increased in prostate cancer tissues, especially in patients at stage III-IV, which was associated with advanced stage and lower overall survival for prostate cancer patients. Furthermore, SNHG14 expressions were increased in prostate cancer cell lines. However, the underlying functions of SNHG14 in prostate cancer remained unclear.

Cyclin D1 is a gene that promotes cell proliferation in cancers[30-32]. N-cadherin and E-cadherin are invasive genes that have been demonstrated to promote cell invasion in multiple cancers[33,34]. Bcl-2, Bax, and Cleaved caspase-3 are important apoptotic genes in the process of apoptosis[35-37]. To explore the role of SNHG14 in the progression of prostate cancer, si-SNHG14 was transfected into DU145 cells, and subsequently the effects of SNHG14 inhibition on proliferation, invasion and apoptosis of DU145 cells were observed. CCK-8 and transwell assay showed that SNHG14 inhibition repressed cell abilities of proliferation and invasion. Flow cytometry revealed that cell apoptotic rate was evaluated following SNHG14 inhibition. WB results showed that the protein levels of Cyclin D1, Bcl-2, and N-cadherin were repressed, while the levels of Bax, Cleaved caspase-3, and E-cadherin were promoted after SNHG14 inhibition. These data suggested that SNHG14 could regulate cell proliferation, invasion, and apoptosis in DU145 cells, while the detailed mechanism remained unknown.

MiRNAs are short RNAs that affect biological functions in cancer[16-18], including prostate cancer[8-11]. It has been demonstrated that lncRNAs can act as a ceRNA to sponge with target miRNAs.

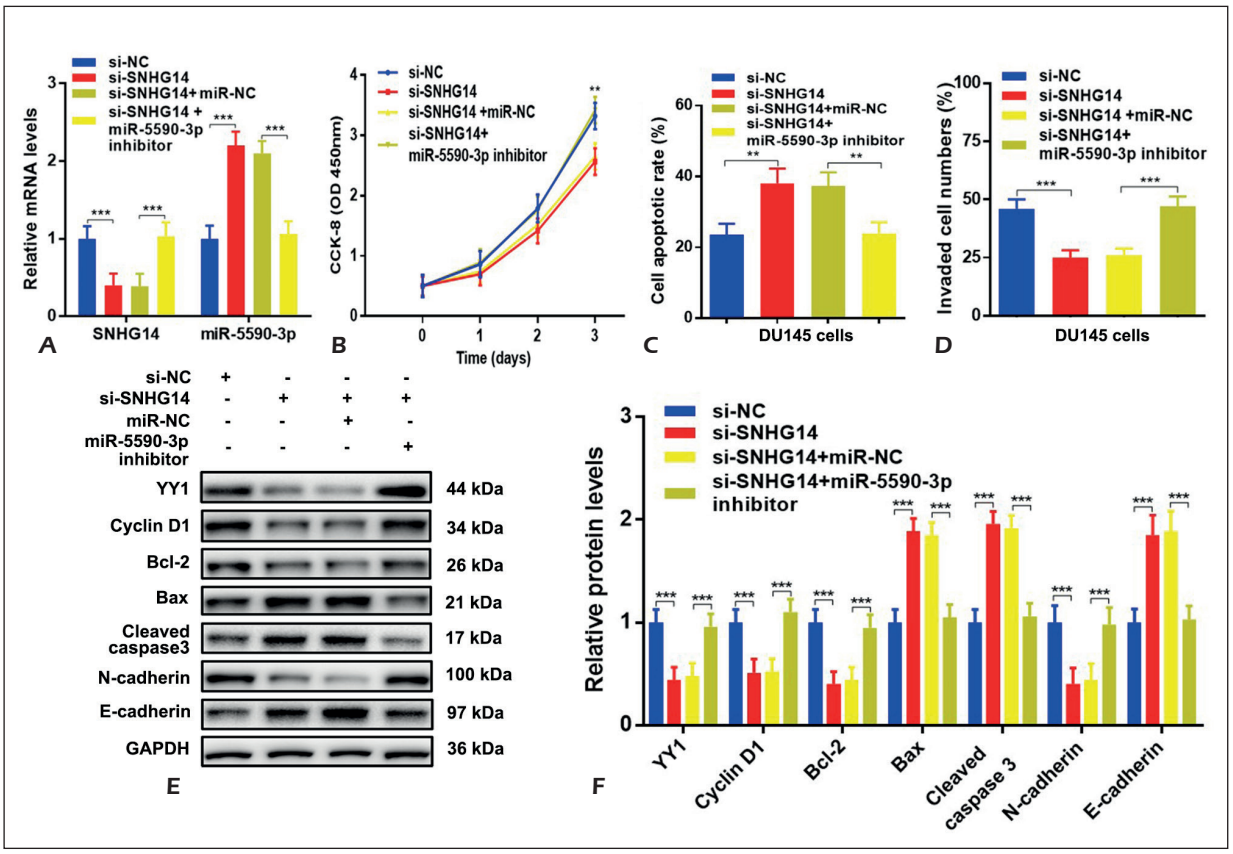

Figure 7. SNHG14 regulated cancer cell growth, apoptosis, and invasion via miR-5590-3p/YY1 axis in prostate cancer. **A**, Expressions of SNHG14 and miR-5590-3p were detected by qRT-PCR. **B**, CCK-8 assay was used to measure cell proliferation abilities. **C**, Cell apoptotic rate was evaluated by flow cytometry. **D**, Invasion abilities were measured by transwell assay. **E-F**, Protein levels of YY1, Cyclin D1, Bcl-2, Bax, Cleaved caspase-3, N-cadherin, and E-cadherin were detected by WB (magnifications: x2.0). $^{**}p<0.001$, $^{***}p<0.001$.

As a result, we used bioinformatics analysis to explore the targets of SNHG14, and miR-5590-3p was predicted as one of the target miRNAs, which was reported to be involved in the progression of some cancers[23-25]. Results showed that miR-5590-3p expression was decreased in prostate cancer tissues, especially in patients at stage III-IV, which was negatively correlated with SNHG14 in prostate cancer tissues and patients at stage of III-IV. These data prompted that SNHG14 was negatively interacted with miR-5590-3p, which was predicted as a downstream molecule for SNHG14. Luciferase reporter assay verified that SNHG14 could directly bind with miR-5590-3p in DU145 cells.

To further explore how did miR-5590-3p regulate prostate cancer cell functions, miR-5590-3p inhibitor was respectively transfected into DU145 cells. CCK-8 and transwell assay showed that miR-5590-3p inhibition promoted cell abilities of proliferation and invasion. Flow cytometry revealed that miR-5590-3p inhibition repressed cell apoptosis. And the protein levels of Cyclin D1, Bcl-2, and N-cadherin were increased, while the levels of Bax, Cleaved caspase-3, and E-cadherin were repressed, suggesting the miR-5590-3p downregulation promoted cell proliferation, invasion, and inhibited apoptosis in DU145 cells. However, the detailed mechanism of miR-5590-3p in prostate cancer was unclear.

To explore how miR-5590-3p regulated cell functions of prostate cancer, TargetScan database was used to predict target genes and YY1 was identified as a potential target gene, which was reported to be an oncogene in some cancers[26-29]. WB results showed that YY1 protein expression was increased in prostate cancer tissues, especially in patients at stage III-IV, which was negatively correlated with miR-5590-3p in prostate cancer tissues and patients at stage of III-IV. These data suggested that YY1 was negatively interacted

with miR-5590-3p. Luciferase reporter assay confirmed that miR-5590-3p could directly bind with the downstream target of YY1 in DU145 cells.

Above all, we might confirm that SNHG14 could function as a ceRNA to sponge with miR-5590-3p, which would repress YY1 expression. To validate our assumption, miR-5590-3p inhibitor was transfected into DU145 cells with si-SNHG14 or si-NC. CCK8 assay and transwell assay showed that the repressed cell proliferation and invasion abilities in si-SNHG14 were reversed followed with miR-5590-3p inhibition. Flow cytometry revealed the promoted cell apoptosis in si-SNHG14 was reversed followed with miR-5590-3p inhibition. Moreover, the protein expressions of YY1, Cyclin D1, Bcl-2, N-cadherin were repressed and Bax, Cleaved caspase-3, and E-cadherin expressions were increased, while they were countervailed followed by miR-5590-3p inhibition. These results confirmed that SNHG14 regulated cancer cell growth, apoptosis, and invasion *via* miR-5590-3p/ YY1 axis in prostate cancer.

Conclusions

We found that SNHG14 was increased in prostate cancer patients, which was related with future diagnosis for prostate cancer patients. Of note, we discovered that SNHG14 could promote cell proliferation, invasion, and repress cell apoptosis *via* miR-5590-3p/YY1 axis in prostate cancer, which might provide a new target for treating prostate cancer.

Acknowledgments

This study was supported by Guangxi Zhuang Autonomous Region Natural Science Foundation (2017gxnsfaa198185), Key Laboratory Construction Project Plan of Guangxi Zhuang Autonomous Region (17-259-57).

Conflict of Interests

The authors declare that they have no conflict of interest.

References

1) Schatten H. Brief overview of prostate cancer statistics, grading, diagnosis and treatment strategies. Adv Exp Med Biol 2018; 1095: 1-14.
2) Gomella LG. Prostate cancer statistics: anything you want them to be. Can J Urol 2017; 24: 8603-8604.
3) Siegel RL, Miller KD, Jemal A. Cancer statistics, 2019. CA Cancer J Clin 2019; 69: 7-34.
4) Siegel RL, Miller KD, Jemal A. Cancer statistics, 2018. CA Cancer J Clin 2018; 68: 7-30.
5) Zhu J, Chen S, Yang B, Mao W, Yang X, Cai J. Molecular mechanisms of lncRNAs in regulating cancer cell radiosensitivity. Biosci Rep 2019; 39. pii: BSR20190590.
6) Tripathi MK, Doxtater K, Keramatnia F, Zacheaus C, Yallapu MM, Jaggi M, Chauhan SC. Role of lncRNAs in ovarian cancer: defining new biomarkers for therapeutic purposes. Drug Discov Today 2018; 23: 1635-1643.
7) Sun Z, Zhang C, Wang T, Shi P, Tian X, Guo Y. Correlation between long non-coding RNAs (lncRNAs) H19 expression and trastuzumab resistance in breast cancer. J Cancer Res Ther 2019; 15: 933-940.
8) Jiang X, Guo S, Zhang Y, Zhao Y, Li X, Jia Y, Xu Y, Ma B. LncRNA NEAT1 promotes docetaxel resistance in prostate cancer by regulating ACSL4 via sponging miR-34a-5p and miR-204-5p. Cell Signal 2020; 65: 109422.
9) Zhang C, Wang GX, Fu B, Zhou XC, Li Y, Li YY. LncRNA CASC15 promotes migration and invasion in prostate cancer via targeting miR-200a-3p. Eur Rev Med Pharmacol Sci 2019; 23: 8303-8309.
10) Wu M, Huang Y, Chen T, Wang W, Yang S, Ye Z, Xi X. LncRNA MEG3 inhibits the progression of prostate cancer by modulating miR-9-5p/QKI-5 axis. J Cell Mol Med 2019; 23: 29-38.
11) You Z, Liu C, Wang C, Ling Z, Wang Y, Wang Y, Zhang M, Chen S, Xu B, Guan H, Chen M. LncRNA CCAT1 promotes prostate cancer cell proliferation by interacting with DDX5 and miR-28-5p. Mol Cancer Ther 2019; 18: 2469-2479
12) Pu J, Wei H, Tan C, Qin B, Zhang Y, Wang A, Wang J. Long noncoding RNA SNHG14 facilitates hepatocellular carcinoma progression through regulating miR-4673/SOCS1. Am J Transl Res 2019; 11: 5897-5904.
13) Jiao P, Hou J, Yao M, Wu J, Ren G. SNHG14 silencing suppresses the progression and promotes cisplatin sensitivity in non-small cell lung cancer. Biomed Pharmacother 2019; 117: 109164.
14) Zhang YY, Li M, Xu YD, Shang J. LncRNA SNHG14 promotes the development of cervical cancer and predicts poor prognosis. Eur Rev Med Pharmacol Sci 2019; 23: 3664-3671.
15) Zhang W, Duan W, Mo Z, Wang J, Yang W, Wu W, Li X, Lin S, Tan Y, Wei W. Upregulation of SNHG14 suppresses cell proliferation and metastasis of colorectal cancer by targeting miR-92b-3p. J Cell Biochem 2019. doi: 10.1002/jcb.29434. [Epub ahead of print].
16) Naeli P, Yousefi F, Ghasemi Y, Savardashtaki A, Mirzaei H. The role of microRNAs in lung cancer: implications for diagnosis and therapy. Curr Mol Med 2019. doi: 10.2174/1566524019666191001113511. [Epub ahead of print].
17) Loh HY, Norman BP, Lai KS, Rahman NMANA, Alitheen NBM, Osman MA. The regulatory role of microRNAs in breast cancer. Int J Mol Sci 2019; 20. pii: E4940.

18) Yang B, Sun L, Liang L. MiRNA-802 suppresses proliferation and migration of epithelial ovarian cancer cells by targeting YWHAZ. J Ovarian Res 2019; 12: 100.

19) Salmena L, Poliseno L, Tay Y, Kats L, Pandolfi PP. A ceRNA hypothesis: the Rosetta Stone of a hidden RNA language? Cell 2011; 146: 353-358.

20) Tay Y, Kats L, Salmena L, Weiss D, Tan SM, Ala U, Karreth F, Poliseno L, Provero P, Di Cunto F, Lieberman J, Rigoutsos I, Pandolfi PP. Coding-independent regulation of the tumor suppressor PTEN by competing endogenous mRNAs. Cell 2011; 147: 344-357.

21) Li Q, Yu Q, Ji J, Wang P, Li D. Comparison and analysis of lncRNA-mediated ceRNA regulation in different molecular subtypes of glioblastoma. Mol Omics 2019; 15: 406-419.

22) Liang W, Sun F. Identification of pivotal lncRNAs in papillary thyroid cancer using lncRNA-mRNA-miRNA ceRNA network analysis. Peer J 2019; 7: e7441.

23) Wu N, Han Y, Liu H, Jiang M, Chu Y, Cao J, Lin J, Liu Y, Xu B, Xie X. miR-5590-3p inhibited tumor growth in gastric cancer by targeting DDX5/AKT/m-TOR pathway. Biochem Biophys Res Commun 2018; 503: 1491-1497.

24) Liang F, Fu X, Wang L. miR-5590-3p-YY1 feedback loop promotes the proliferation and migration of triple-negative breast cancer cells. J Cell Biochem 2019; 120: 18415-18424.

25) Zhang W, Wu Y, Hou B, Wang Y, Deng D, Fu Z, Xu Z. A SOX9-AS1/miR-5590-3p/SOX9 positive feedback loop drives tumor growth and metastasis in hepatocellular carcinoma through the Wnt/β-catenin pathway. Mol Oncol 2019; 13: 2194-2210.

26) Zhu G, Qian M, Lu L, Chen Y, Zhang X, Wu Q, Liu Y, Bian Z, Yang Y, Guo S, Wang J, Pan Q, Sun F. O-GlcNAcylation of YY1 stimulates tumorigenesis in colorectal cancer cells by targeting SLC22A15 and AANAT. Carcinogenesis 2019. doi: 10.1093/carcin/bgz010. [Epub ahead of print].

27) Huang T, Wang G, Yang L, Peng B, Wen Y, Ding G, Wang Z. Transcription factor YY1 modulates lung cancer progression by activating lncRNA-PVT1. DNA Cell Biol 2017; 36: 947-958.

28) Hays E, Bonavida B. YY1 regulates cancer cell immune resistance by modulating PD-L1 expression. Drug Resist Updat 2019; 43: 10-28.

29) Li X, Yu M, Yang C. YY1-mediated overexpression of long noncoding RNA MCM3AP-AS1 accelerates angiogenesis and progression in lung cancer by targeting miR-340-5p/KPNA4 axis. J Cell Biochem 2019. doi: 10.1002/jcb.29448. [Epub ahead of print].

30) Holah NS, Hemida AS. Cyclin D1 and PSA act as good prognostic and clinicopathological indicators for breast cancer. J Immunoassay Immunochem 2019: 1-17.

31) Ramos-García P, González-Moles MÁ, González-Ruiz L, Ayén Á, Ruiz-Ávila I, Bravo M, Gil-Montoya JA. Clinicopathological significance of tumor cyclin D1 expression in oral cancer. Arch Oral Biol 2019; 99: 177-182.

32) Zhong Q, Hu Z, Li Q, Yi T, Li J, Yang H. Cyclin D1 silencing impairs DNA double strand break repair, sensitizes BRCA1 wildtype ovarian cancer cells to olaparib. Gynecol Oncol 2019; 152: 157-165.

33) Cao ZQ, Wang Z, Leng P. Aberrant N-cadherin expression in cancer. Biomed Pharmacother 2019; 118: 109320.

34) Labernadie A, Kato T, Brugués A, Serra-Picamal X, Derzsi S, Arwert E, Weston A, González-Tarragó V, Elosegui-Artola A, Albertazzi L, Alcaraz J, Roca-Cusachs P, Sahai E, Trepat X. A mechanically active heterotypic E-cadherin/N-cadherin adhesion enables fibroblasts to drive cancer cell invasion. Nat Cell Biol 2017; 19: 224-237.

35) Saffari Chaleshtori J, Heidari-Sureshjani E, Moradi F, Heidarian E. The effects of thymoquinone on viability, and anti-apoptotic factors (BCL-XL, BCL-2, MCL-1) in prostate cancer (PC3) cells: an in vitro and computer-simulated environment study. Adv Pharm Bull 2019; 9: 490-496.

36) Ahagh MH, Dehghan G, Mehdipour M, Teimuri-Mofrad R, Payami E, Sheibani N, Ghaffari M, Asadi M. Synthesis, characterization, anti-proliferative properties and DNA binding of benzochromene derivatives: Increased Bax/Bcl-2 ratio and caspase-dependent apoptosis in colorectal cancer cell line. Bioorg Chem 2019; 93: 103329.

37) Zhao YY, Wu Q, Wu ZB, Zhang JJ, Zhu LC, Yang Y, Ma SL, Zhang SR. Microwave hyperthermia promotes caspase3-dependent apoptosis and induces G2/M checkpoint arrest via the ATM pathway in non-small cell lung cancer cells. Int J Oncol 2018; 53: 539-550.